INVESTIGATION OF THE CUT-OFF FREQUENCY OF 500µm MMIC GAN HEMT DEVICE AT 10V, 16V AND 20V DRAIN VOLTAGES FROM 1-25 GHz

AKWURUOHA C. N.
Department of Electrical/Electronic Engineering
Michael Okpara University of Agriculture Umudike
Umuahia, Nigeria
Email: akwuruoha.charles@mouau.edu.ng

ABSTRACT

This paper presents an investigation of the cut-off frequency of 500 µm (4 x 125 µm) monolithic microwave integrated circuit (MMIC) gallium nitride high electron mobility transistor (GaN HEMT) device at 10V, 16V and 20V drain voltages from 1 to 25 GHz. The GaN HEMT device was fabricated by WIN Semiconductor using NP25-00 0.25 µm GaN HEMT process. S-parameter measurement was carried out with vector network analyzer (VNA) while the simulation was carried out with Keysight advanced design system software (ADS) from 1 to 25 GHz at gate voltage of -2V and drain supply voltages of 10V, 16V and 20V respectively. The measured and simulated results were compared at 5 GHz. The S-parameter results were used to compute the transistor current gain and determine the cut-off frequency of the MMIC GaN HEMT device. The cut-off frequency of the measured MMIC GaN HEMT device from 1 to 25 GHz and drain supply voltages of 10V, 16V and 20V respectively stood at 19 GHz, 23 GHz and 23.9 GHz whereas the cut-off frequency of the simulated MMIC GaN HEMT device stood at 20 GHz, 18 GHz and 17.6 GHz.

Keywords: *GaN HEMT; device; S-parameter; drain voltage; cut-off frequency*

I. INTRODUCTION

Wide band gap gallium nitride high electron mobility transistor (GaN HEMT) finds application in devices where there is desirability for high power handling capability, high switching speed, high thermal conductivity and high electron drift velocity (Akwuruoha, 2018). The use of wideband GaN HEMT devices is limited by the inability of GaN HEMT devices to operate at frequencies higher than 10 GHz due to low cut-off frequency. This has further underscored the need to determine the cut-off frequency of GaN HEMT transistor devices by comparing the simulation and measurement results. This comparison will enable the RF and microwave circuit designers to make an accurate and informed decision in RF circuit design. While some workers have extensively carried out some works in GaN HEMT (Mishra *et al*, 2002), (Green *et al*, 2000), (Pengelly *et al*, 2012), (Okamoto, et al, 2004), (Green *et al*, 2000), (Mishra *et al*, 2008), (Darwish *et al*, 2004), (Shen *et al*, 2001), (Aaen *et al*, 2007), (Dunleavy *et al*, 2010), (Fager *et al*, 2002), (Wood and Root, 2004), (Kazior and Wu, 2008), the use of measured and simulated S-parameter results to compute such transistor figure of merit such as small signal current gain (H_{21}) and determine the cut-off frequency of 500µm GaN HEMT device has yet to be investigated as proposed in this paper. This paper is organized as follows. Section II discusses the theory of GaN HEMT device including S-parameter and transistor figures of merit. Section III discusses the measurement and simulation results. Section IV concludes the paper.

II. THEORY

A. GaN HEMT

Gallium nitride high electron mobility transistor is produced through the process of metallic beam epitaxy (MBE) or metallic organic chemical vapour deposition (MOCVD) (Mishra *et al*, 2002). The comparison of the electrical characteristics wideband GaN HEMT with other semiconductors including such transistor figures of merit as Baliga's figure of merit (BFOM) and Johnson's figure of merit (JM) have been reported by Okamoto *et al*, 2004 as shown in Table 1.

Table 1. Electrical characteristic of GaN HEMT showing Baliga's and Johnson's Figure of merit

Material	Mobility(μ) $cm^2/V.s$	Band Gap E_g (eV)	Break Down Field (E_b) 10^6 V/cm	BFOM Ratio	JM
Si	1300	11.9	0.3	1.0	1.0
GaAs	5000	12.5	0.4	9.6	2.7
4H-SiC	260	10	3.5	3.1	20
GaN	1500	9.5	2	24.6	27.5

B. S-Parameter and Transistor Figures of Merit

1) S-Parameter

The S-parameter [S] of a two-port network is derived from the reflection and transmission coefficients to and from the transistor device between the source and the load as reported by Bahl (2009) and Pozar (2012). The S-parameters results used in this paper were obtained through measurement using a vector network analyzer (VNA) or by simulation of the modeled device using a computer added design software. In this work, keysight's advanced design system (ADS) has been used to carry out the S-parameters simulations. The measured and simulated S-parameters include: Input Reflection Coefficient (S_{11}), Output Reflection Coefficient (S_{22}), Forward Transmission Coefficient (S_{21}) and Reverse Transmission Coefficient (S_{12}). A two-port network with an arbitrary source impedance (Z_S), load impedance (Z_L), source reflection coefficient (Γ_S), input reflection coefficient (Γ_{IN}), output reflection coefficient (Γ_{OUT}) and load reflection coefficient (Γ_L) is shown in Figure 1.

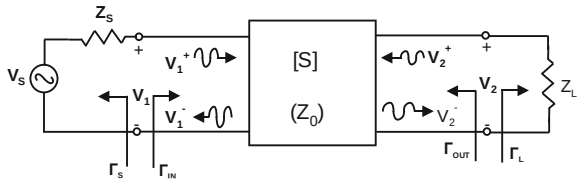

Figure 1. A two-port network with an arbitrary source and load

2) Transistor Figures of Merit

The transistor figures of merit discussed in this paper include: small signal current gain (H_{21}), Maximum stability gain (MSG) and maximum available gain (MAG). The H_{21}, MSG and MAG are obtained using the measured/simulated transistor S-parameters (Akwuruoha, 2018), (Cheng, 2005), (Pawlikiewicz and Hess, 2006), Ahn *et al*, 2004.

a) Small Signal Current Gain (H_{21})

The small signal current gain of transistor can be defined in accordance with S-parameters as

$$H_{21} = \frac{-S_{21}}{(1-S_{11})(1+S_{22})+S_{12}S_{21}} \quad (1)$$

Where S_{21} is forward transmission coefficient, S_{12} is the reverse transmission coefficient, S_{11} is the input reflection coefficient and S_{22} is the output reflection coefficient.

b) Maximum Stable Gain (MSG)

The maximum stable gain is defined as

$$MSG = \left|\frac{S_{21}}{S_{12}}\right| \quad (2)$$

c) Maximum Available Gain (MAG)

The maximum available gain is defined as

$$MAG = \left|\frac{S_{21}}{S_{12}}\right|\left(K \pm \sqrt{K^2 - 1}\right) \quad (3)$$

where K is Rollet's stability factor (Jackson, 2006), (Tan *et al*, 2009):

$$K = \frac{1 - |S_{11}|^2 - |S_{22}|^2 + \Delta^2}{2|S_{12}S_{21}|} > 1 \quad (4)$$

Where, $$|\Delta| = |S_{11}S_{22} - S_{12}S_{21}| < 1 \quad (5)$$

III. RESULTS AND DISCUSSION

The investigation of the cut-off frequency of the GaN HEMT proposed in this paper is presented in accordance with drain supply voltage of the transistor device at 10V, 16V and 20V from 1GHz to 25 GHz frequency and gate voltage of -2V.

A. Measured and Simulated Result at drain voltage of 10V from 1-25 GHz.

S-parameter measurement and simulation of the fabricated and modeled 500µm GaN HEMT carried out at drain supply voltage of 10V from 1 to 25 GHz indicates that the fabricated GaN HEMT has measured S_{11} of -2.3 dB and S_{22} of -8.2 dB whereas the simulated model S_{11} of -1.3 dB and S_{22} of -5.4 dB as shown in the linear graph and Smith chart in Figures 2 and 3. Similarly, the fabricated device has measured $S_{21}$of 8.1 dB and S_{12} of -20.1 dB whereas the simulated model has S_{21} of 12 dB and S_{12} of -28.4 dB as shown in the linear graph and Smith chart in Figures 4 and 5.

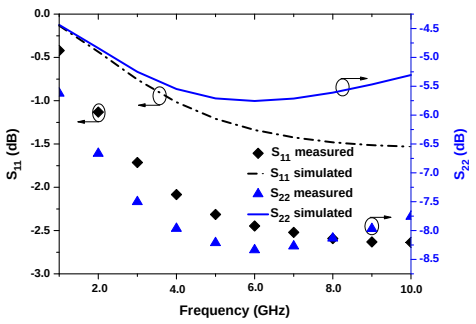

Figure 2. S_{11} and S_{22} at drain voltage of 10V from 1-25 GHz

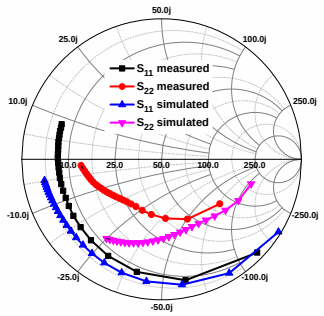

Figure 3. Smith Chart of S_{11} and S_{22} at drain voltage of 10V

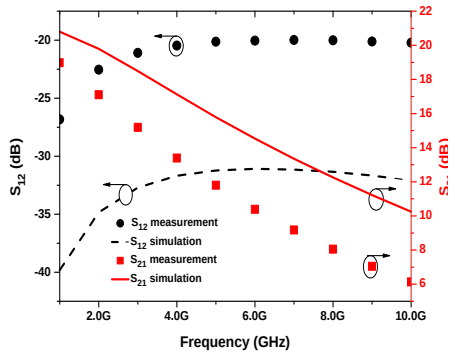

Figure 4. S_{12} and S_{21} at drain voltage of 10V from 1-25 GHz

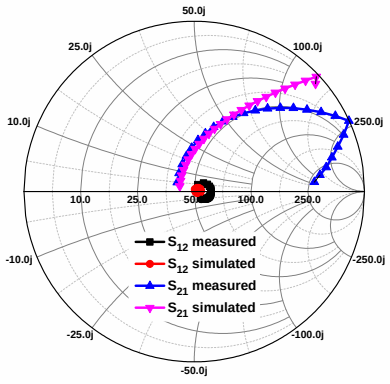

Figure 5. Smith Chart of S_{12} and S_{21} at drain voltage of 10V from 1-25 GHz

The cut-off frequency (F_T) is the frequency at which the small signal current gain is zero. The small signal current gain (H_{21}) for the measured (H_{21m}) and simulated (H_{21s}) device indicates cut-off frequency of 19 GHz and 20 GHz respectively as shown in Figure 6.

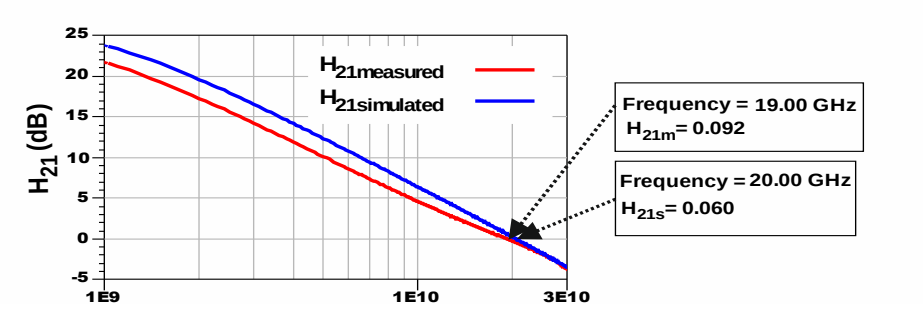

Figure 6. Small signal current gain of the GaN HEMT at drain voltage of 10V

B. Measured and Simulated Result at drain voltage of 16V from 1-25 GHz.

S-parameter measurement and simulation of the fabricated and modeled 500µm GaN HEMT device were respectively carried out at drain supply voltage of 16V from 1 to 25 GHz in order to determine the cut-off frequency defined as the frequency at which the small signal current gain is zero. The result indicates that the fabricated GaN HEMT has measured S_{11} of -1.9 dB and S_{22} of -6.4 dB whereas the simulated model has S_{11} of -1.1 dB and S_{22} of -3.1 dB as shown in the linear graph and Smith chart in Figures 7 and 8 respectively.

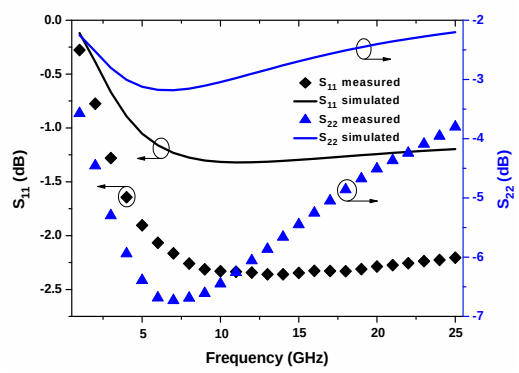

Figure 7. S_{11} and S_{22} at drain drain voltage of 16V from 1-25 GHz

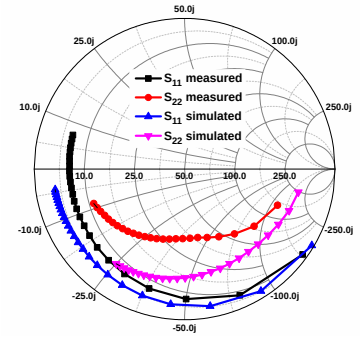

Figure 8. Smith Chart showing S_{11} and S_{22} at drain drain voltage of 16V from 1-25 GHz

The fabricated GaN HEMT has measured S_{21} of 13.6 dB and S_{12} of -23.4 dB whereas the simulated model has S_{21} of 15.9 dB and S_{12} of -34.5 dB as shown in the linear graph and Smith chart in Figures 9 and 10 respectively.

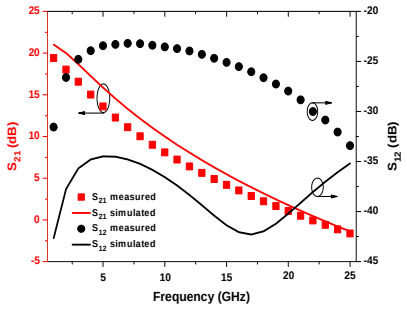

Figue 9. S_{12} and S_{21} at drain drain voltage of 16V from 1-25 GHz

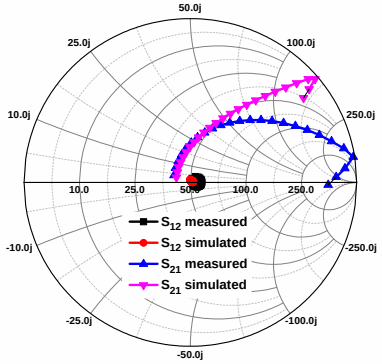

Figure 10. Smith chart of S_{12} and S_{21} at drain drain voltage of 16V from 1-25 GHz

The small signal current gain (H_{21}) for the measured (H_{21m}) and simulated (H_{21s}) device indicates F_t of 23 GHz and 18 GHz respectively as shown in Figure 11.

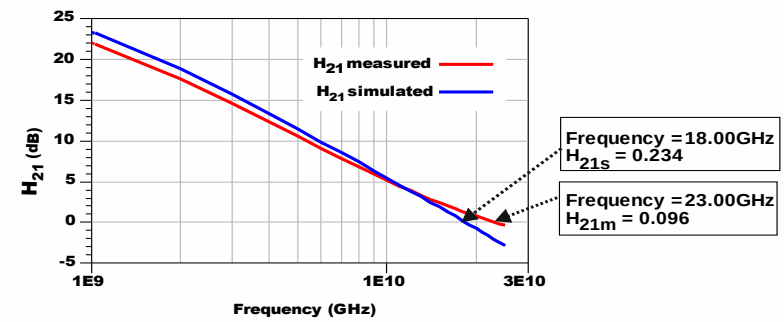

Figure 11. Small signal current gain and cut-off frequency at drain voltage of 16V from 1-25 GHz

C. Measured and Simulated Result at drain voltage of 25V from 1-25 GHz.

S-parameter measurement and simulation of the fabricated and modeled 500µm GaN HEMT device were respectively carried out at drain supply voltage of 25V from 1 to 25 GHz in order to determine the cut-off frequency defined as the frequency at which the small signal current gain is zero. The results compared at 5 GHz indicate that the fabricated GaN HEMT has measured S_{11} of -1.8 dB and S_{22} of -5.3 dB whereas the simulated model has S_{11} of -1.1 dB and S_{22} of -3.1 dB as shown in the linear graph and Smith chart in Figures 12 and 13 respectively.

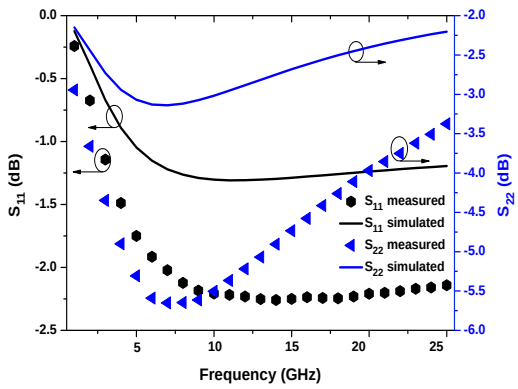

Figure 12. S_{11} and S_{22} at drain voltage of 20V from 1-25 GHz

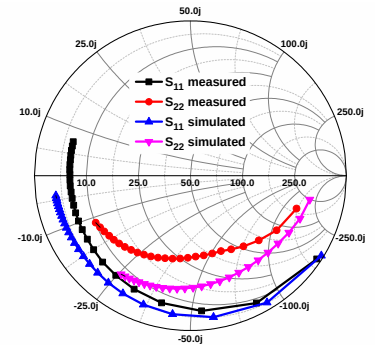

Figure 13. Smith chart of S_{11} and S_{22} at drain drain voltage of 20V from 1-25 GHz

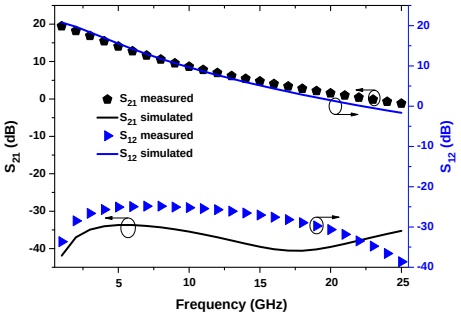

Figure 14. S_{12} and S_{21} at drain voltage of 20V from 1-25 GHz

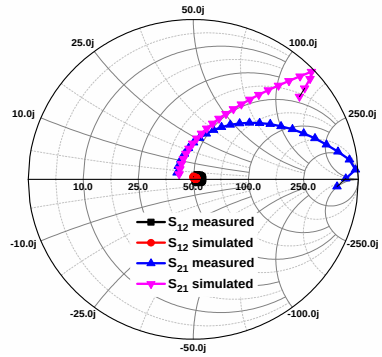

Figure 15. Smith chart of S_{12} and S_{21} at drain drain voltage of 20V from 1-25 GHz

The fabricated GaN HEMT has measured S_{21} of 14.1 dB and S_{12} of -235.1 dB whereas the simulated model has S_{21} of 15.5 dB and S_{12} of -33.7 dB as shown in the linear graph and Smith chart in Figures 14 and 15 respectively.

The small signal current gain (H_{21}) for the measured (H_{21m}) and simulated (H_{21s}) device indicates F_t of 23.9 GHz and 17.6 GHz respectively as shown in Figure 16.

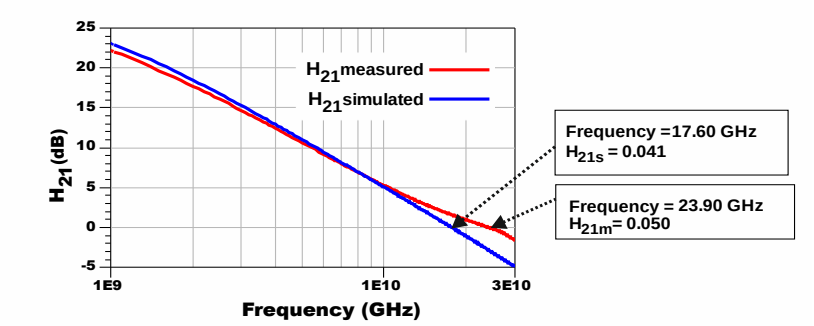

Figure 16. Small signal current gain and cut-off frequency at drain voltage of 20V from 1-25 GHz

IV. CONCLUSION

S-parameter measurement and simulation of the fabricated and modeled WIN Semiconductor 500µm GaN HEMT device carried out from 1 to 25 GHz at drain supply voltages of 10V, 16V, 20V and gate voltage of -2V show good agreement regarding the results which were used to compute the small signal current and determine the cut-off frequency. The frequency at which the small signal current gain equals zero is the cut-off frequency of the GaN HEMT device. The results validate the cut-off frequency of the WIN 500µm GaN HEMT device being investigated in this paper at drain supply voltages of 10V, 16V and 20V. The cut-off frequency result will be valuable to RF and microwave circuit designers.

V. ACKNOWLEDGMENT

The author is grateful to WIN Semiconductors Incorporation for providing the model GaN HEMT device used in this work. The author is also grateful to The University of Manchester Microwave Laboratory for VNA measurement.

REFERENCES

Aaen, P. H., Pla, J. A. and Wood, J. (2007). Modeling and Characterization of RF and Microwave Power FETs. Cambridge University Press, Cambridge, United Kingdom.

Ahn, J., Yun, H., Lim, S., Lee, H., Park, S., Lee, H., Kang, Y., Kim, D., and Lee, S. (2004). Novel Method for Accurate Extraction of F_{max} for Nano-Scale MOSFETs. Journal of Phys. Society, 45(5), pp. 1201-1204.

Akwuruoha, C. N. (2018). Modelling and Design of Non-Foster Class-J Power Amplifier for Wireless Communication Systems. PhD Dissertation, The University of Manchester, Manchester, United Kingdom.

Bahl, I. J. (2009). Fundamental of RF and Microwave Transistor Amplifiers. John Wiley and Sons Inc, New Jersey, USA, pp. 34.

Cheng, Y. (2005). A Study of Figures of Merit for High Frequency Behaviour of MOSFETs in RFIC Applications. NSTI-Nanotech, pp. 81-86.

Darwish, A. M., Bayba, A. and Hung, H. A. (2004). Thermal resistance calculation of AlGan/GaN devices. *IEEE Trans. Microw. Theory Tech.*,52(11), pp. 2611–2620.

Dunleavy, L., Baylis, C., Curtice, W. and Connick, R. (2010). Modeling GaN: Powerful but challenging. *IEEE Microw. Mag.*, pp.83–96.

Mishra, U.K., Parikah, P. and Wu, Y. F. (2002). AlGaN/ GaN HEMTs-An Overview of Device Operation and Applications. Proceedings of the IEEE, 90(6), pp. 1022-1031.

Fager, C., Pedro, J. C., de Carvalho, N. B. and Zirath, H. (2002). Prediction of IMD in LDMOS transistor amplifers using a new large-signal model. IEEE Trans. Microw. Theory Tech., 50(12), pp. 2834–2842.

Green, B. M., Chu, K. K., Chumbes, E. M., Smart, J. A., Shealy, J. R. and Eastman, L. F. (2000). The effect of surface passivation on the microwave characteristics of undoped AlGaN/GaN HEMTs. *IEEE Electron Device Lett.*, 21(6), pp. 268–270.

Green, B.M., Chu, K. K., Chumbes, E. M., Smart, J. A.,Shealy, J. R. and Eastman, L. F. (2000).The effect of surface passivation on the microwave characteristics of undoped AlGaN/GaN HEMTs. *IEEE Electron Device Lett.*, 21(6), pp. 268–270.

Jackson, R. W. (2006). Rollet Proviso in the Stability of Linear Microwave Circuits- A Tutorial. IEEE Transactions on Microwave Theory and Techniques, 54(3), pp. 993-1000.

Kazior, T. E. and Wu, Y. F. (2008). GaN-Based RF Power Devices and Amplifier. IEEE, 96(2), pp. 287-303.

Kuzuhara, M. (2004). Improved power performance for a recessed-gate AlGaN–GaN heterojunction FET with a field-modulating plate.

IEEE Trans. Microw. Theory Tech., 52(11), pp. 2536–2540.

Okamoto, Y., Ando, Y., Hataya, K., Nakayama, T., Miyamoto, H., Inoue, T., Senda, M., Hirata, K., Kosaki, M., Shibata, N. and Mishra, U. K., Shen, L., Kazior, T. E. and Wu, Y. F. (2008). GaN Based RF Power Devices and Amplifier. Proc. IEEE, 96(2), pp. 287-303.

Pawlikiewicz, A. H. and Hess, D. (2006). Choosing RF CMOS or SiGe BiCMOS in mixed-signal design. RF Design, pp. 36-44.

Pengelly, R. S., Wood, S. M., Milligan, J. W., Sheppard, S. T. and Pribble, W.L. (2012). A Review of GaN on SiC High Electron Mobility Power Transistors and MMICs. IEEE Transactions on Microwave Theory and Techniques, 60(6), pp. 1764-1783.

Pozar, D. M. (2012). Microwave Engineering. John Wiley and Sons Inc, New Jersey, 4th Edition, pp. 559.

Shen, L., Heikman, S., Moran, B., Coffe, R., Zhang, N. Q., Buttari, D., Smorchkova, I. P., Keller, S., DenBaars, S. P. and U. K. Mishra, U. K. (2001). AlGaN/AlN/GaN high-power microwave HEMT. *IEEE Electron Device Lett.*,22(10), pp. 457–459.

Tan, L., Sun, X., and Ang, K. S. (2009). Unconditional Stability Criteria for Microwave Networks. PIERS Proceedings, Beijing, China, pp. 1524-1528.

Wood, J. and Root, D. (2004). A symmetric and thermally-de-embedded nonlinear FET model for wireless and microwave applications. *IEEE MTT-S Int. Microw. Symp. Dig.*, pp. 35–38.